INTERPOLATION AND PRESTACK DATA ENHANCEMENT USING PARTIAL I-CRS STACK

M. Koushesh, B. Schwarz, and D. Gajewski

email: *mohsen.koushesh@zmaw.de*

keywords: *5-D interpolation, pre-stack data enhancement, data regularization*

ABSTRACT

During seismic data acquisition a lot of reasons can cause loss of traces or the loss of desired signals because of noise. In this study, interpolation, regularization and enhancement of signal to noise ratio in seismic data are considered using CRS and i-CRS attributes. After introducing the partial i-CRS and reviewing the partial CRS stack, we evaluate their abilities in recovering signals. In our work-flow, we test both methods on simple and complex synthetic data examples. Both operators showed similar results in recovering lost reflection signals, but in case of diffractions, the partial i-CRS stack extracted higher amplitude seismic signals even at large offsets when compared with partial CRS stacking. The coherency factor of the partial i-CRS stack also provided a higher value which makes the determination of CRS attribute more reliable than using the CRS method.

INTRODUCTION

Lack of permission for exploration in special areas, damaged receivers or high noise levels in some seismograms during filed data acquisition are some problems which may require interpolation, regularization and/or to enhance the signal to noise ratio. This part of data processing gets more crucial when we know that the outputs of this stage, will be the base of other stages in seismic data processing. Regularization of traces and filling data gaps are usually performed using different binning and interpolation techniques (see, e.g., Brune et al. (1994), Yilmaz (2001), Stolt (2002), Fomel (2003), Spitzer et al. (2003), Chandola et al. (2004), Herrmann et al. (2008)). Based on the CRS method (Common Reflection Surface) Baykulov and Gajewski (2008, 2009), created new powerful stacking based interpolation technique called partial CRS stack which can be also used to improve the quality of pre-stack data by incorporating information not only from neighboring traces in the offset dimension but also from neighboring CMPs. Performed on 3-D data it corresponds to a 5-D interpolation method (inline, crossline, offset, azimuth, time) where the dips of the events are automatically considered.

It has be shown previously Schwarz (2011) that the i-CRS operator better fits reflection seismic data than the CRS operator. The improvement is particularly significant for diffractions. CRS attributes play a key role for wavefield separation, e.g., to separate diffractions from reflections. So far it has been successfully applied in the post-stack domain (Dell and Gajewski, 2011). The separation process in the pre-stack domain is based on partial stacks (see the report by Baktiari et al. in this volume). Therefore we are also interested in the performance of the i-CRS operator for partial stacks. Since i-CRS provides improved CRS attributes the partial stack method should benefit from that. Since the i-CRS does not contain zero offset time it would require a different implementation than the CRS operator. Therefore we consider the shifted version of the i-CRS operator as used by Schwarz (2011). The shifted version of the i-CRS operator is particularly suited for applications since it can be easily incorporated into the existing code for partial CRS stacking. In the next sections we schematically show the differences of stacking surface and partial stacking surface over our data cube. Afterwards, by giving some synthetic data examples, we evaluate the power of both

operators in filling data gaps and enhancing the signal to noise ratio in pre-stack data. For this goal, we consider two simple models including a single reflector and diffractor. Finally we apply the methods to the data of the Sigsbee 2A synthetic model.

THE I-CRS OPERATOR IN OPTICAL-IMAGE-SPACE

After introducing the i-CRS operator by Vanelle et al. (2010) which presents a double square root expression for reflection traveltimes, Schwarz et al. (2013) extended the operator to heterogeneous media by an effective medium approach and suggested an alternative version of the i-CRS operator in the optical-image-space. We obtain the optical image space version from the effective-medium i-CRS operator by applying the following procedure:

1- Replace the actual zero-offset traveltime t_0 by its optical analogue

$$t_p = \frac{2R_{nip}}{v_0} \tag{1}$$

Where R_{nip} is radii of curvature of the normal-incidence-point wave and v_0 is the near surface constant velocity.

2- Subtract the time shift $t_p - t_0$ from the total traveltime t.

By applying the instructions to the i-CRS operator, we obtain the shifted version of i-CRS:

$$t - t_0 + \frac{2R_{nip}}{v_0} = t_s(v_0, \alpha, R_{nip}, R_n) + t_g(v_0, \alpha, R_{nip}, R_n) \tag{2}$$

Where R_n is the radius of curvature of the normal wave, α is the emergence angle of the ZO ray, t is total traveltime, t_s denotes a part of traveltime from the source to the reflection point and t_g the part of the traveltime from the reflection point to the receiver:

$$t_s = \frac{1}{v_0} \sqrt{(\Delta x_m - h + R_n \sin\alpha - (R_n - R_{nip})\sin\theta)^2 + (R_n \cos\alpha - (R_n - R_{nip})\cos\theta)^2} \tag{3}$$

$$t_g = \frac{1}{v_0} \sqrt{(\Delta x_m + h + R_n \sin\alpha - (R_n - R_{nip})\sin\theta)^2 + (R_n \cos\alpha - (R_n - R_{nip})\cos\theta)^2} \tag{4}$$

The angle θ is obtained from the recursive equation:

$$\tan\theta = \frac{\Delta x_m + R_n \sin\alpha}{R_n \cos\alpha} + \frac{h}{R_n \cos\alpha} \frac{t_s - t_g}{t_s + t_g} \tag{5}$$

The presence of t_s and t_g in this equation emphasizes the implicit character of the operator which inspired its name. It was shown previously (Vanelle et al., 2010; Schwarz, 2011) that ignoring the second term or assuming $t_s = t_g$ in Eq. 5 leads to a sufficient accuracy of the resulting traveltimes. This simplifies the application and implementation of the i-CRS operator.

THE PARTIAL STACKING SURFACE

After the determination of stacking parameters for each zero offset traveltime and for each CMP, we sum the data along the red net shown in Figure 1, which defines the i-CRS stacking surface over the defined apertures in offset and midpoint dimensions. For the stack we assigns the result to the corresponding zero offset point $B = (t_0, 0)$. In partial stacking we may consider just a part of the i-CRS surface (blue net) and assign the stacking result to any position on this surface. We may assign the stack result to, e.g., the sample $A(t_h, h)$, where t_h is two way traveltime and h is half source-receiver offset. In other words: We may interpolate the waveforms to any position on the partial stack surface. In this understanding the partial stack concept is the most universal stacking concept were the stack to zero offset and time is just a special case.

To implement the partial stack for each sample $A(t_h, h)$, a search procedure selects the best t_0 and determines the resulting i-CRS parameters which result in the minimum time deviation from t_h at the offset h. For the selection process, we restrict our choices to pre-defined values of coherency. This leads
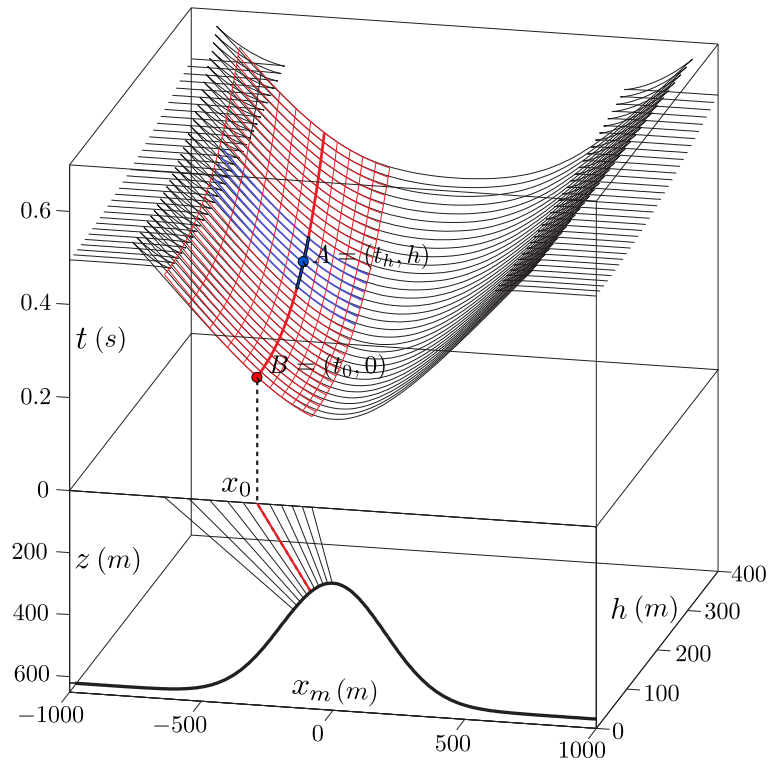
Figure 1: i-CRS stacking surface (red net) which belongs in point $B = (t_0, 0)$ and Partial i-CRS stacking surface (blue net) which is assigned to point $A = (t_h, h)$. Modified Müller (1999).

to a filtering which considers only those events which are above the pre-defined threshold. By assuming that α, R_{nip} and R_n vary smoothly in the vicinity of event A, these selected parameters are kept fixed to compute t_0 from the traveltime t_h and offset h in equation (2), i.e.:

$$t_0 = t_h - t_s(v_0, \alpha, R_{nip}, R_n) - t_g(v_0, \alpha, R_{nip}, R_n) + \frac{2R_{nip}}{v_0} \qquad (6)$$

The computed t_0 together with its corresponding stacking parameters are used in equation (2) to construct the partial i-CRS stacking surface which fits the considered event A.

SIMPLE SYNTHETIC DATA TESTS

To evaluate the performance of the partial i-CRS stack, we designed two simple synthetic models which include a single curved reflector with curvature radius of 10 km (Model REF) and a "point" diffractor with a curvature radius of 10 m (Model DIF), where both structures are located at a minimum depth of 1 km. For both models we assumed an inhomogeneous overburden comprising a constant vertical velocity gradient of $0.5\ s^{-1}$ and a near surface velocity of $2000\ ms^{-1}$. Figure 2(a) and 2(b) schematically depict the designed models. For the modeling of the synthetic data we choose a receiver interval of $25m$ and a maximum offset of $2\ km$. The CMP fold is 81. The total extend of the data acquisition is $5km$ and the sampling interval is $4ms$. In the first numerical experiment, Gaussian noise with a signal to noise ratio (S/N) of 5 is added to the data. In the examples we compare the results of the partial stack based on the CRS and i-CRS operators.

Figure 3 shows the results of partial stacking for Model REF and DIF, respectively, where we have interpolated the traces by partial stacks exactly at the positions of the seismograms of the input data. The results for Model REF are displayed in the left column and the results for Model DIF are shown in the right column. The top row displays the input seismograms, the middle row the CRS partial stacks and the bottom row the i-CRS partial stacks. The pre-stack data enhancement effect of the partial stacks is
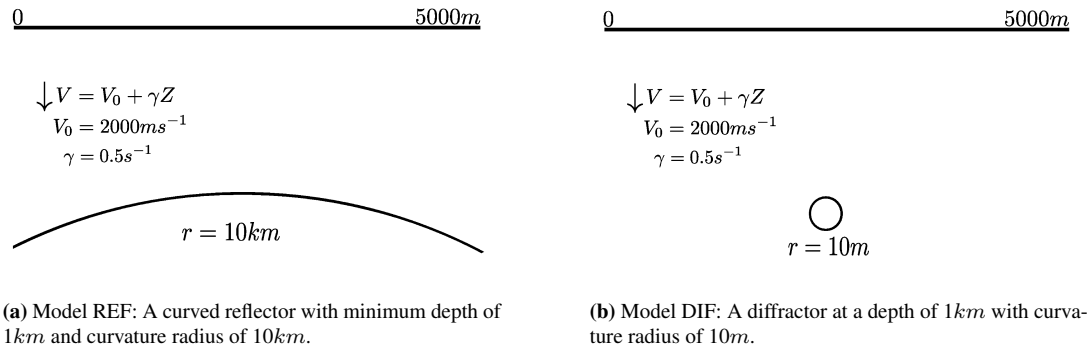
0 _____ 5000m   0 _____ 5000m

$\downarrow V = V_0 + \gamma Z$
$V_0 = 2000 ms^{-1}$
$\gamma = 0.5 s^{-1}$

$\downarrow V = V_0 + \gamma Z$
$V_0 = 2000 ms^{-1}$
$\gamma = 0.5 s^{-1}$

$r = 10km$

$r = 10m$

(a) Model REF: A curved reflector with minimum depth of $1km$ and curvature radius of $10km$.

(b) Model DIF: A diffractor at a depth of $1km$ with curvature radius of $10m$.

Figure 2: Simple synthetic models with inhomogeneous overburden. For details see text.

clearly visible since the S/N ratio is considerably improved. The waveforms are very well reconstructed for most offsets, even for offsets considerably larger than the target depth. There are a few distortions in the waveforms which may be a problem in the current implementation of the method. For Model REF the differences between CRS and i-CRS are hardly visible. Stronger differences are observed for the diffraction case (Model DIF) in the right column. Particularly at large offset the i-CRS operator better reconstructs the recorded diffracted waveforms. This is in accordance with previous results that the i-CRS operator better fits the data of diffractions at large offsets when compared to CRS. This conclusion obviously also concerns the quality of the attributes.

In a second numerical experiment we included three data gaps at three different offset areas in our simple synthetic data. These gaps are at short offsets, intermediate offsets, i,.e., with an offset to target ratio close to one, and at large offsets with an offset to target ratio close to two. The latter is already outside the "hyperbolic window". With this experiment we can investigate the behavior of the partial stacks at different offsets. No noise was added to data in this case since the pre-stack data enhancement effect was already demonstrated in the previous example. In the left column of Figure 4 the results for model REF are displayed. The right column shows the results for model DIF. The top row shows the input data, middle row the CRS partial stacks, and the bottom row presents the i-CRS partial stack results.

For model REF again hardly any differences can be detected. Even at the large offset data gap no clear differences between the partial CRS and i-CRS stack can be recognized. For this case the CRS attributes are well determined even outside the hyperbolic window for both methods. Again, the diffraction case give a different results. Whereas the partial i-CRS stack reconstructs the waveforms well even at the large offset data gaps, the CRS partial stack amplitudes are decreased. In the next section we consider a complex synthetic example displaying a lot of diffractions because of rough topography of the top of salt.

COMPLEX SYNTHETIC DATA TESTS

In this numerical study we apply both methods in the complex synthetic Sigsbee 2A model. Because of the rough topography of the top of salt we observe a large number of diffractions in the stack leading to numerous conflicting dip situations. Sigsbee 2A is a 2-D synthetic data set, simulating the geological structure of Golf of Mexico. The model does not contain free surface multiples. This synthetic model is a constant density acoustic data set. Figure 5 shows the optimized CRS stack. CRS and i-CRS attributes were determined using Mann (2002)'s code modified to include the CRS and i-CRS operator. Similar to the simple models, we evaluate the partial CRS and i-CRS stacks in two separate experiments: In the first case, we add Gaussian noise to original synthetic data such that events are not visible. We reconstruct the data at exactly the same positions of the input seismograms. In the second case we consider data gaps at different offset ranges.

Figure 6(a) and 6(b) shows CMP gathers at CMP position 800. On the left the raw data are shown, on the right the same data after adding Gaussian noise are displayed. It is almost impossible to identify events in this gather. Figure 6(c) and 6(d) show the partial CRS and i-CRS stack results. Despite the extremly poor data quality of the input gather, both partial stack results display proof the powerful pre-stack data enhancement feature of these methods. Both partial stacks do not reconstruct the small amplitude events
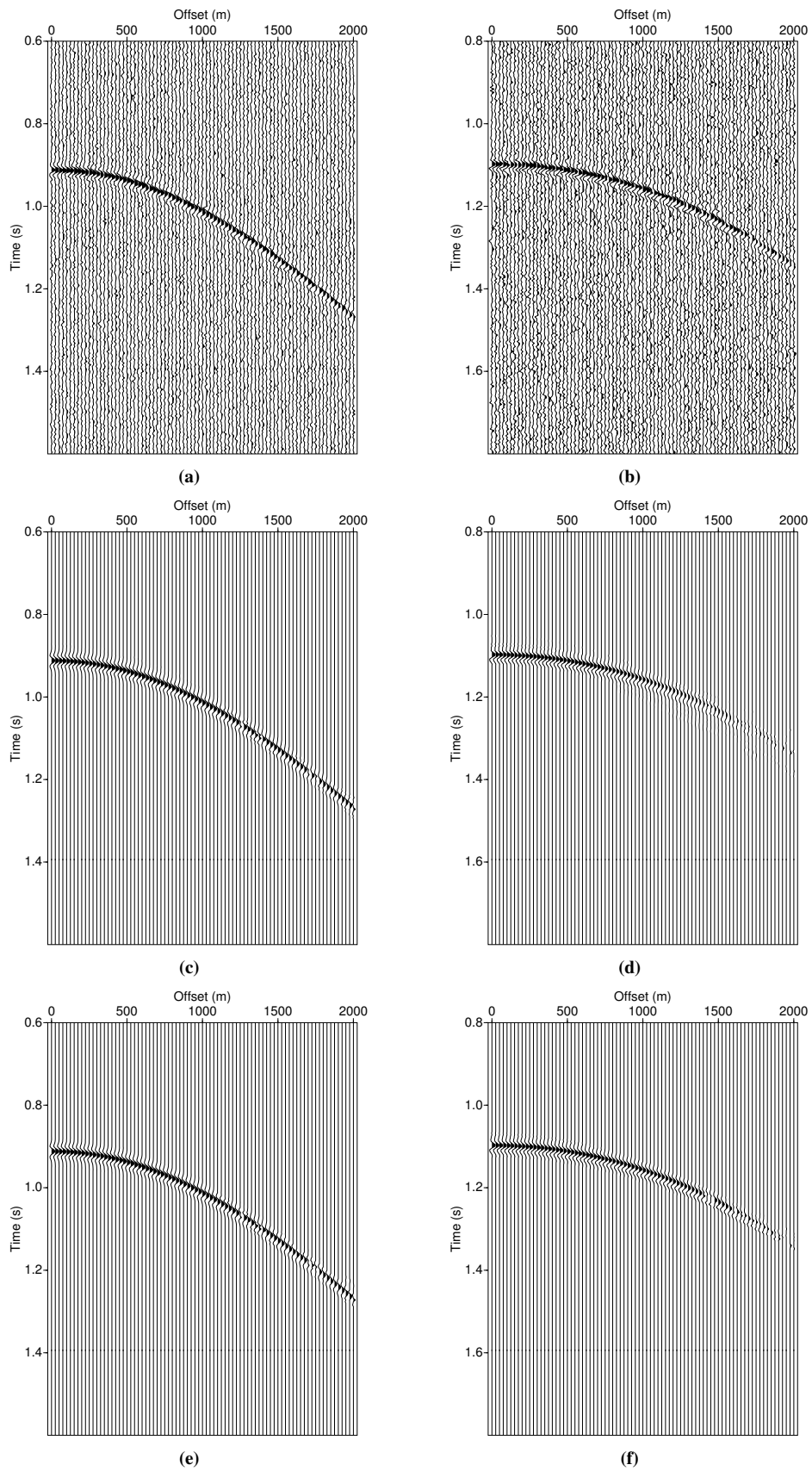
Figure 3: (a) Input data for Model REF at CMP 3250 m. (b) Input data for Model DIF at CMP 3250 m. (c) CRS partial stack Model REF, (d) CRS partial stack Model DIF, (e) i-CRS partial stack Model REF, (f) partial i-CRS stack Model DIF.
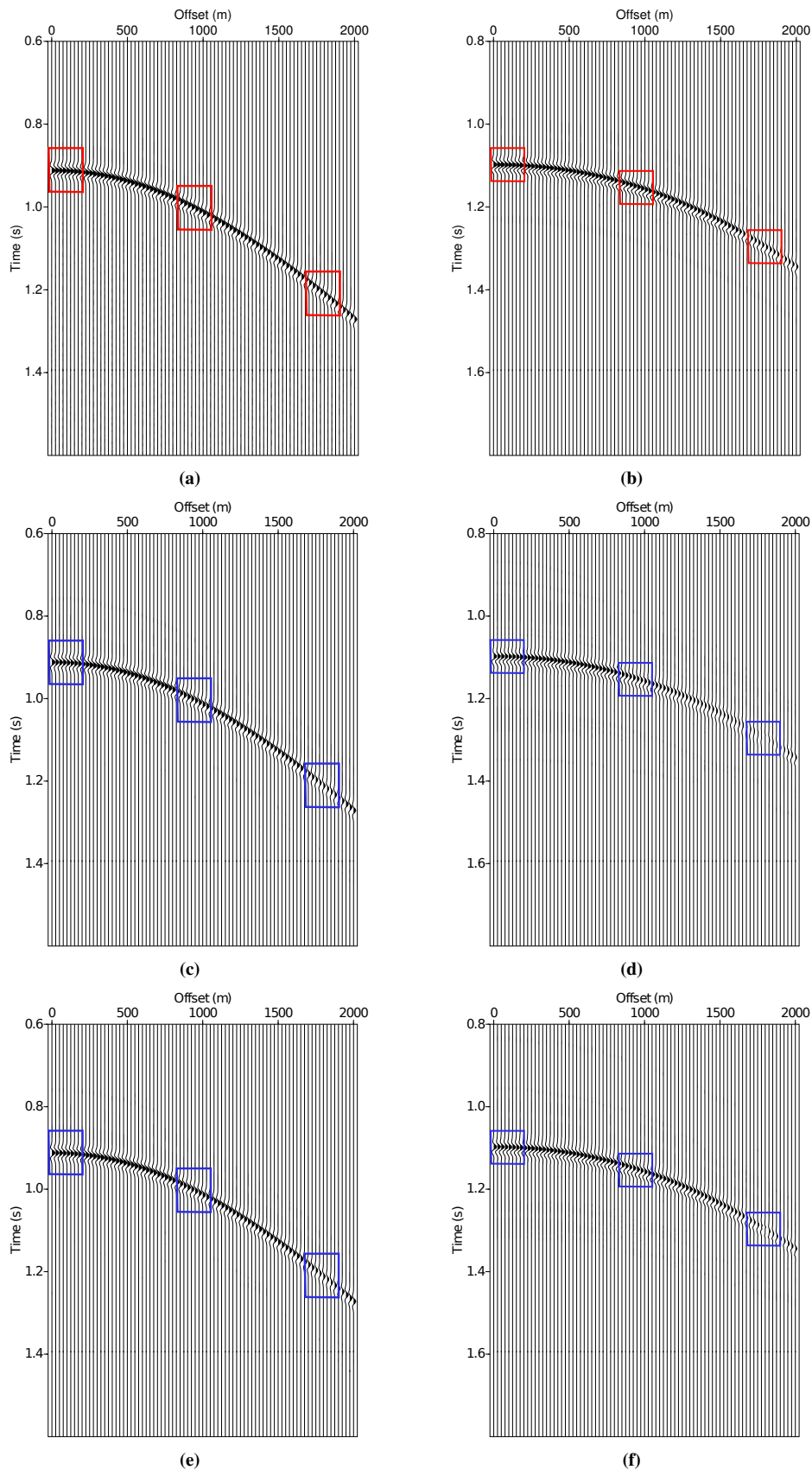
Figure 4: (a) CMP gather for model REF comprising three data gaps at three different offsets. (b) same as (a) but for model DIF. (c) Partial CRS stack results for input (a). (d) Partial CRS stack for input (b). (e) Partial i-CRS stack for input (a). (f) Partial i-CRS stack for input (b). Red boxes in (a) and (b) indicate location of gaps and the original waveforms before removal. In figures (c), (d), (e) and (f) the blue boxes show the interpolated signals).
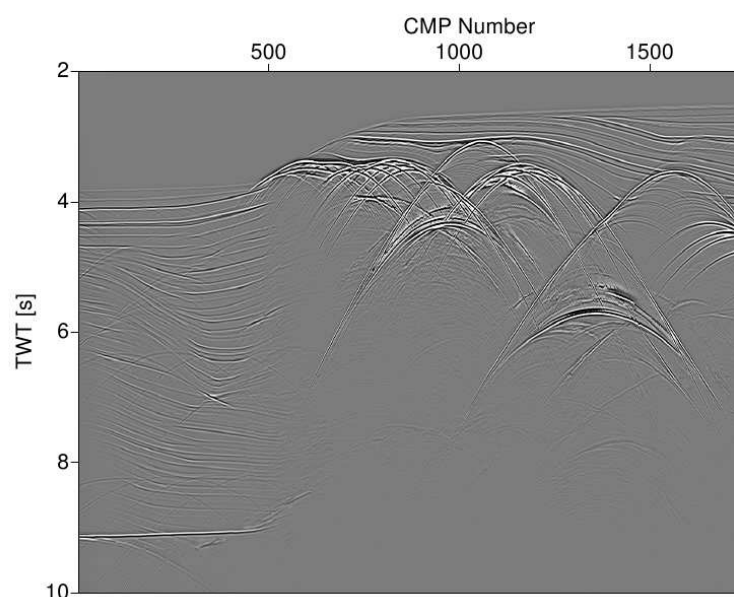
Figure 5: CRS stack of the Sigsbee 2A data set.

at TWT greater than 4.1 s only visible in the noise-free data (Fig. 6(a)) but not recognizable in the actual input gather (Fig. 6(b)). This is an effect of the coherence threshold and the strong noise used in this experiment. The i-CRS shows more events, i.e., i-CRS better fits the data resulting in a higher coherence above the threshold and allowed to reconstruct events not present in the CRS partial stack. Both partial stacks, however, show also distortions in the waveforms which is an unwanted side effect of the coherence threshold in the current implementation. The coherence is not constant for all samples of an event and parts may be not included in the partial stack. This is currently further investigated and a more sophisticated implementation of the coherence threshold will resolve this issue.

In the second example we introduce again missing traces at various offsets of the noise free data and reconstruct the data with both partial stack methods. Figure 7(a) and 7(b) show the input data at CMP number 800 before and after introducing the gaps, respectively. Figure 7(c) and 7(d) show the partial CRS and i-CRS stack results. Because of the much better S/N ration in this case also the small amplitude events at larger TWT are reconstructed. There are differences between the CRS and i-CRS partial stacks related to weak events. Apparently i-CRS better fits the data and leads to higher coherence values above the threshold. Otherwise both results look very similar.

CONCLUSIONS

In this study we introduced the partial i-CRS stack and compared it to the already established partial CRS stack method. We considered generic simple synthetic models resembling the reflection and diffraction case as well as a complex synthetic model comprising a lot of diffractions and conflicting dip situations. Both partial stack methods display a powerful pre-stack data enhancement quality. They showed similar results in recovering reflection signals hidden in noise, but in case of diffractions, the partial i-CRS stack was superior in extracting higher amplitudes of lost signals even at large offsets. Because of better data fit and coherency factors the partial i-CRS stack recovered more signals than the CRS partial stack method. Both techniques show sometimes distortions in the waveforms which is an unwanted side effect of the coherence threshold used in the partial stacks. This, however, is not a feature of the method but an issue of the implementation and thresholding. Although the partial stack was already established within the CRS workflow its extension to the i-CRS is an essential advancement. Because of the better performance with diffraction, the i-CRS method is clearly preferred. The better attributes will lead to a better separation of reflections and diffractions in the stack (see, e.g., Dell and Gajewski (2011)). For the separation in the pre-
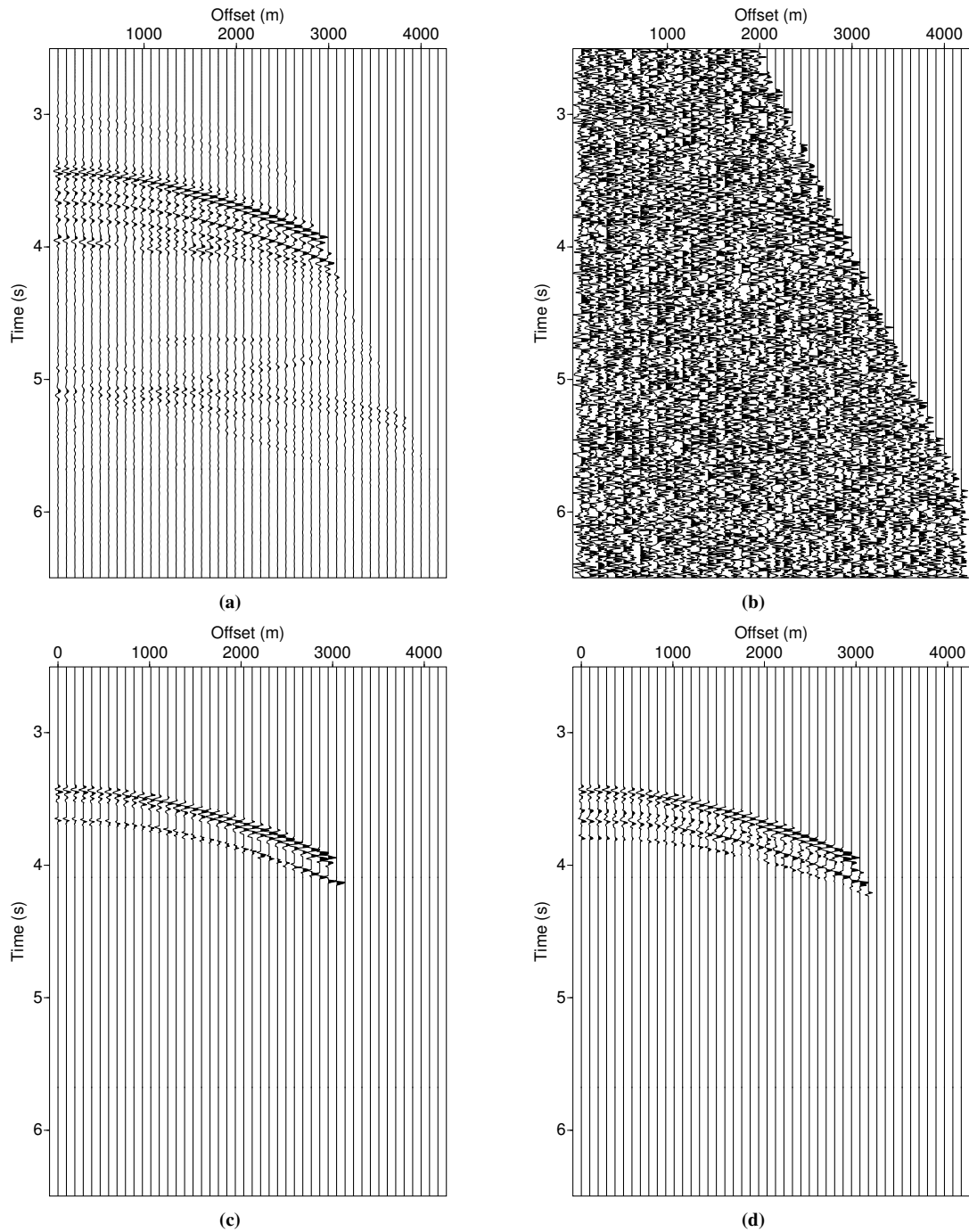
Figure 6: (a) Data at CMP number 800 for the Sigsbee 2A data before adding noise. (b) Input gather after adding Gaussian noise. (c) Result of partial CRS stack. (d) Result of partial i-CRS stack.
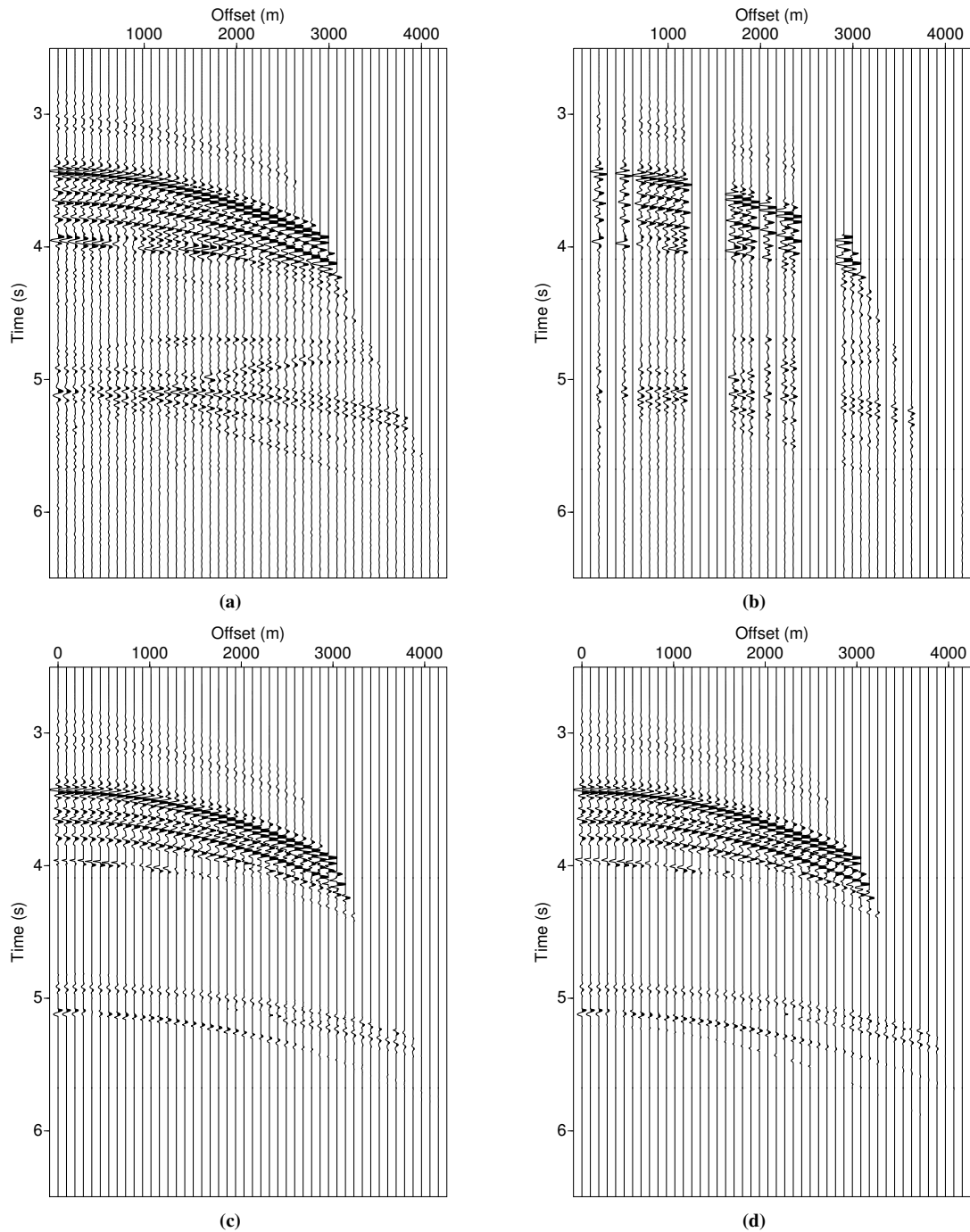
Figure 7: (a) Data at CMP number 800 for the Sigsbee 2A data before removing traces. (b) The same after removing some traces. (c) Reconstructed traces by partial CRS stack. (d) Reconstructed traces by partial i-CRS stack.

stack domain, the partial stack is the tool of choice (see paper by Baktiari et al in this volume). The better performance of the i-CRS operator for diffractions will support the pre-stack separation of reflections from diffractions.

ACKNOWLEDGMENTS

REFERENCES

Baykulov, M. and Gajewski, D. (2008). Seismic data enhancement with common reflection surface (crs) stack method. *Soc. Expl. Geophys. Expanded Abstracts*.

Baykulov, M. and Gajewski, D. (2009). Prestack seismic data enhancement with partial common reflection surface (crs) stack. *Geophysics*, 74(3):V49–V58.

Brune, R. H., O'Sullivan, B., and Lu, L. (1994). Comprehensive analysis of marine 3-dbin coverage. *The Leading Edge*, 13:757–762.

Chandola, S. K., Singh, V., Saha, A., Sarma, P. L. N., Rao, M. P., and Ramakrishna, K. (2004). Seismic surveying in an urban setting. *The Leading Edge*, 23:1078–1082.

Dell, S. and Gajewski, D. (2011). Common-reflection-surface-based workflow for diffraction imaging. *Geophysics*, 76(5):S187–S195.

Fomel, S. (2003). Seismic reflection data interpolation with differential offset and shot continuation. *Geophysics*, (68):733–744.

Herrmann, F. J., Wang, D., Hennenfent, G., and Moghaddam, P. P. (2008). Curvelet-based seismic data processing: A multiscale and nonlinear approach. *Geophysics*, 73:A1–A5.

Mann, J. (2002). *Extensions and Applications of the Common-Reflection-Surface Stack Method*. PhD thesis, University of Karlsruhe.

Müller, T. (1999). *The Common Reflection Surface Stack Method: Seismic Imaging without explicit knowledge of the velocity model*. PhD thesis, University of Karlsruhe.

Schwarz, B. (2011). A new nonhyperbolic multi-parameter stacking operator. Master's thesis, Hamburg University.

Schwarz, B., Vanelle, C., and Gajewski, D. (2013). Auxiliary media – a generalized view on stacking. In press.

Spitzer, R., Nitsche, F. O., Green, A. G., and Horstmeyer, H. (2003). Efficient acquisition, processing, and interpretation strategy for shallow 3d seismic surveying: A case study. *Geophysics*, 68:1792–1806.

Stolt, R. H. (2002). Seismic data mapping and reconstruction. *Geophysics*, 67:890–908.

Vanelle, C., Kashtan, B., Dell, S., and Gajewski, D. (2010). A new stacking operator for curverd subsurface structures. *SEG, Expanded Abstracts*, 29:3609–3613.

Yilmaz, O. (2001). *Seismic data analysis - Processing, inversion, and interpretation of seismic data*. Society of Exploration Geophysicists.